Robotica (2005) volume 23, pp. 491–499. © 2005 Cambridge University Press
doi:10.1017/S0263574704001043 Printed in the United Kingdom

Multi-loop model-based control structure for robot manipulators

Rafael Osypiuk*, Bernd Finkemeyer† and Friedrich M. Wahl†

(Received in Final Form: September 9, 2004)

SUMMARY

Most nonlinear control concepts used in robotics are based on a more or less accurate inverse model of the robot. In contrast to this, the design and properties of a general n-loop control structure based on a divided forward model of the robot, the so-called multi-loop Model Following Control Structure (n-MFC), is presented in this paper. Its theoretical basics and its concept are explained. The stability and robustness of the proposed control structure is analyzed. The theoretical assumptions are verified in many experiments with a two-joint robot manipulator. Qualitative as well as quantitative results of the experiments are presented and discussed.

KEYWORDS: Control structure; Multi-loop model; Two-joint robot.

I. INTRODUCTION

Physical phenomena occurring in nature are strongly nonlinear in the majority of cases, which obviously exerts an effect, directly or indirectly, on properties of processes to be controlled. Static and dynamic nonlinearities exhibited by the controlled process frequently are accompanied by time-variant process parameters, which makes the classic single-loop PID control systems ineffective to cope with such processes. As remedy, employing adaptive algorithms is suggested in the literature.[1] Those, however, suffer from being expensive and difficult to implement. Hence, a search for novel solutions, that would combine simplicity and easiness of tuning offered by classic single-loop PID control structures with an increased resistance to process perturbations becomes a matter of topical interest. These expectations could be met by the Model Following Control (MFC) structure, the properties of which have been analysed thoroughly in reference [2, 3]. Results of tests that had been carried out on MFC when applied to an electro-heating process and robot control were reported in reference [4] and [5], respectively. Although being much more resistant to process perturbations than the classic PID feedback system, MFC still suffers from a limitation due to its single model loop. The limitation is due to the fact, that employing a complete dynamic process model in MFC turns out to be impossible when a strongly nonlinear process is dealt with in reference [6]. To alleviate the problem, the obvious thing to do would be dividing the process model into n parts, which leads to creating a n-loop MFC structure and eliminates the above-mentioned limitation.

Corresponding author: B. Finkemeyer. E-mail: B.finkemeyer@tu-bs.de
† Institute for Robotics and Process Control, Technical University of Braunschweig, Mühlenpfordtstr. 23, 38106 Braunschweig (Germany).
* Institute of Control Engineering, Technical University of Szczecin, ul. 26 Kwietnia 10, 70-313 Szczecin (Poland).

II. ESSENTIAL PROPERTIES OF THE n-MFC STRUCTURE

To give a better insight into the advantages the generalized n-MFC structure offers, let us look on the operation principle of the two-loop MFC structure (Fig. 1). The structure can be divided into a pre-simulated control loop and a process loop with PID algorithms used for control. The former loop consists of a dynamic process model M_1 and its linear controller R_1, the output of which is brought to the process input. The latter loop includes the process plant P together with its corrective controller R_k, which is driven by an error produced as a difference between the model output y_{m1} and the process output y. The difference may arise from modeling inaccuracies, effects of system disturbances z etc. Thus, the summed action produced by both controllers, i.e. R_1 and R_k, excites the input of the real process plant P. The MFC structure may be described by the following transfer function:

$$y = y_{m1}\frac{P(1 + R_k M_1)}{M_1(1 + R_k P)} + \frac{1}{1 + R_k P}\, z \qquad (1)$$

where

$$y_{m1} = y_o \frac{R_1 M_1}{1 + R_1 M_1}.$$

Examining the above-mentioned control concept brings up the following question: How the control performance provided by MFC is influenced by the model accuracy? The commonly adopted rule says, "the more accurate is the model, the better". This is the case, for example, when a reverse model in a feedforward control system is employed. However, MFC requires another way of looking at the problem. The reason has to do with the single PID control loop, which embraces the model. Since the controller R_1 is characterized by a limited resistance to the model nonlinearity, its transfer function should be adopted so as to ease the task the corrective controller R_k has to perform on the one hand, and to secure the required control performance in the first MFC loop on the other hand. The problem is important, because the model output is tracked directly by the process output. So, for example, if we have to deal with an overshoot in the first loop, the other loop will also exhibit an overshoot of the same value or even bigger.

https://doi.org/10.1017/S0263574704001043 Published online by Cambridge University Press

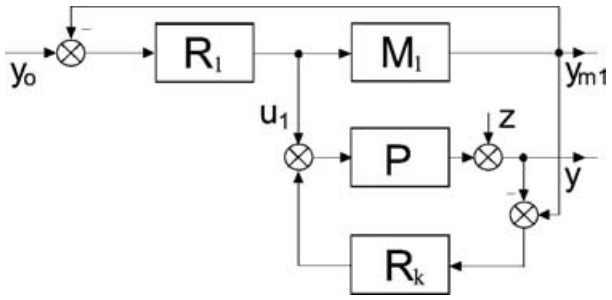


Fig. 1. Structure of the MFC system.

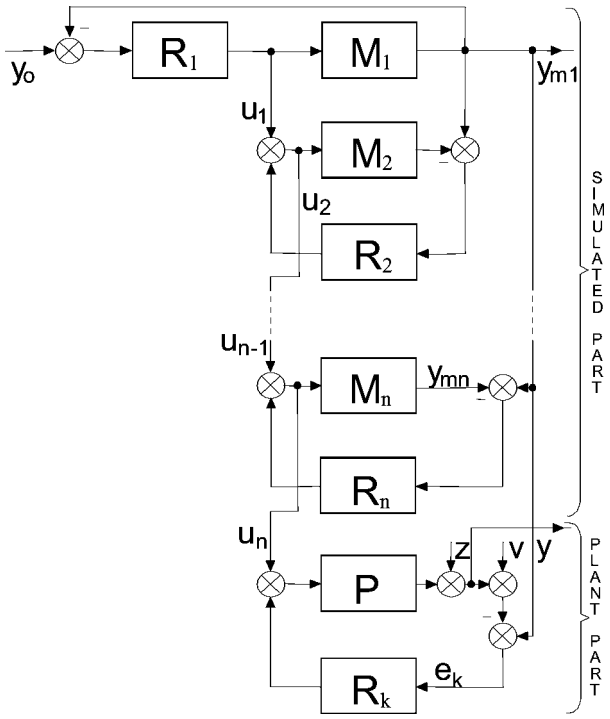


Fig. 2. The n-MFC structure.

The described phenomenon is directly associated with the model complexity. Thus, the two-loop MFC structure should be rearranged so as to employ the entire mathematical model of the process. The solution of this issue lies in the way the process model is written. It is customary to assume that the model consists of a nonlinear static part and a linear dynamic one. Thus, for a wide class of processes it may be written as:

$$x_{out} = \underbrace{f_d\left(x_{in1}(t), x_{in2}(t), \ldots\right)}_{\textit{dynamic part}} + \underbrace{f_s\left(x_{in1}(t), x_{in2}(t), \ldots\right)}_{\textit{static part}}. \quad (2)$$

The conventional two-loop MFC structure is expanded by an additional PID loop. Figure 2 depicts the general form of the resulting structure. The first loop consists of an incomplete model, i.e. the dynamic part $f_d(x)$, and its controller R_1 that has to work out a manipulated variable u_1 for the dynamic part of the model. This variable is applied directly to the input of the complete model equation (2) in the second loop, the controller R_2 of which is relieved of acting on the dynamic part and is engaged in control of the static part only. The nonlinear manipulated variables u_1 and u_2 after being added up are applied to the process input, where the corrective controller R_k adjusts the process by comparing the output of the first model y_{m1} and the process output y. In doing so, the adverse effect of disturbances or model inaccuracy is reduced. Thus, the three-loop 2-MFC with a two-loop model structure secures a much better control performance than that achieved in the case of the classic two-loop MFC. This is due to the possibility of producing more strongly nonlinear manipulated variables.

Thus, the presented control concept is practicable in case, the nonlinear static part and the dynamic process model admit separation. This raises the question of how to proceed when the separated parts of the model are such highly nonlinear that they do not reach control performance to be obtained in the simulated loops. So, there exists a class of processes for which a graduation of the model complexity is possible. The general case may be written as:

$$\begin{aligned} M_1 &= m_1 \\ M_2 &= m_1 + m_2 \\ &\vdots \\ M_i &= m_1 + m_2 + \ldots + m_i \\ &\vdots \\ M_n &= m_1 + m_2 + \ldots + m_i + \ldots + m_n \end{aligned} \quad (3)$$

where m_i are nonlinear parts of the process model M_n. An example of such a process is a serial manipulator. In its construction parts that are dependent on inertia, velocity (centrifugal and Coriolis torques), gravitation and friction forces can be distinguished. For the strong nonlinearity of individual terms employing the classic PID control or even the two-loop MFC may be insufficient to ensure a desired control performance. Here a useful aid can be provided by employing a multi-loop n-MFC structure, which may be depicted for the model (3) in the following way.

The structure of Fig. 2 is composed of n model loops determined by the number of accessible nonlinear terms in the mathematical process model. The transfer function for pre-simulated loops in the case of $i \geq 2$ has the form:

$$y_{m_n} = \left(\frac{M_n\left(1 + M_1 R_2\right)}{M_1 \prod_{i=2}^{n}\left(1 + M_i R_i\right)} + \sum_{i=3}^{n} \frac{M_n R_i}{\prod_{i}^{n}\left(1 + M_i R_i\right)} \right) y_{m_1} \quad (4)$$

where

$$y_{m_1} = y_o \frac{M_1 R_1}{1 + M_1 R_1}.$$

The advantage of using pre-simulated loops in the n-MFC system can be easily seen by considering the diagram of Fig. 2. The first completely independent loop of the proposed structure includes a simplest process model M_1 along with its linear controller R_1. The necessity of gaining the best possible control performance in this loop should be emphasized here, because the first loop serves as an exemplar not only for the consecutive model loops, but also for the last process P loop. For this reason a linear dynamic model M_1 should be employed here. The next loop includes the

https://doi.org/10.1017/S0263574704001043 Published online by Cambridge University Press

model M_2, which consists of the model of the preceding loop plus the new nonlinear part of the model. As may be seen, the i-th controller R_i acts on the i-th part of the model m_i only. In this way partial manipulated variables u_i are created that form eventually the nonlinear manipulated variable u_n, which represents an input to the process P. Since the process may be affected by disturbances and the model is only an approximate one, a corrective controller is added to the last loop. The transfer function of the n-MFC system in presence of system disturbances z and output-related disturbances v has the following form:

$$y = \frac{P}{M_n(1+PR_k)} y_{m_n} + \ldots \\ \ldots + \frac{PR_k}{1+PR_k} y_{m_1} - \frac{PR_k}{1+PR_k} v + \frac{1}{1+PR_k} z. \quad (5)$$

From eq. (5) the influence of the corrective controller R_k becomes clear. It is identical with that of the single-loop PID system. A compromise is needed while tuning the R_k gain for the reason of system stability, since for $R_k \gg 1$ the output-related disturbances v, i.e. noise caused by measuring transducers, are not suppressed, even though the process output then perfectly tracks the reference signal, and the influence the system disturbances z exert is of minor character. The compromise may be worked out by experiments.

III. ROBUSTNESS OF THE PROPOSED CONTROL STRUCTURE

Process variability can be modeled in different ways:[7] As a multiplicative uncertainty Δ_m, or as an additive Δ_a, viewed from both input and output of the nominal plant. If the nominal model of the actual process P is designated as M_n, then the multiplicative model of uncertainty viewed from the process output (also called relative error[8]) is defined by:

$$\Delta_m = \frac{P - M_n}{M_n} = \frac{P}{M_n} - 1 = \frac{\Delta_a}{M_n} \quad (6)$$

By appropriate manipulations eq. (5) may be divided into its model part and its process part. In view of eq. (6), the output of the perturbed n-MFC system takes the form:

$$y = \underbrace{\frac{(1+\Delta_m)M_nR_1}{1+(1+\Delta_m)M_nR_k}}_{T_k} \cdot \underbrace{\frac{M_1(F+M_nR_k)}{M_n(1+M_1R_1)} y_o}_{y_0'} \quad (7)$$

It can be rewritten as:

$$y\left\{1+(1+\Delta_m)M_nR_1\left(\frac{R_k}{R_1}\right)\right\} = y_0'(1+\Delta_m)M_nR_1 \quad (8)$$

Equation (8) corresponds to the block diagram of Fig. 3.

Assuming that Δ_m, the nominal control system (process loop), and the model loops are asymptotically stable, then the following inequality is taken as the necessary and sufficient condition for asymptotic stability of the perturbed n-MFC system:

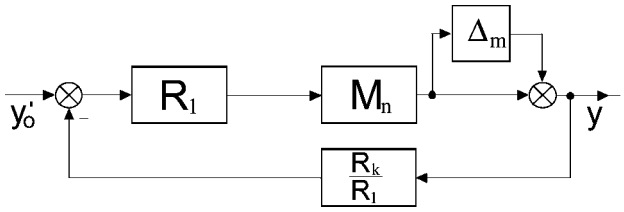


Fig. 3. Equivalent block diagram of the n-MFC system for the purpose of robustness analysis.

$$|\Delta_m| < \frac{|1+M_nR_k|}{|M_nR_1|} = \frac{1}{|T_k|} \quad (9)$$

It may be easily noted, that getting greater robustness of n-MFC through a greater R_k gain is accompanied by better y_o tracking or good suppression of system disturbances. Thus, if for two different controllers $R_{k1} > R_{k2}$ and the same M_n the following inequality holds true,

$$\left[\frac{|1+M_nR_{k1}|}{|M_nR_1|}\right]_{(a)} > \left[\frac{|1+M_nR_{k2}|}{|M_nR_1|}\right]_{(b)} \quad (10)$$

then the control loop (a) exhibits a greater robustness than that of loop (b).

The above presented robustness features of an n-MFC system might be worth to compare with the classic single-loop structure, for which the necessary and sufficient conditions for asymptotic stability of a perturbed system take the form[7]

$$|\Delta_m|_{PID} < \frac{|1+M_1R_1|}{|M_1R_1|} = \frac{1}{|T_{class}|}. \quad (11)$$

As may be inferred from (11), in order to allow great values of Δ_m, the maximal value of $|T_{class}|$ should be lowered as far as possible. This is due to the necessity of "slowing down" the R_1 controller operation by reducing its gain. However, this leads to impaired y_o tracking and impaired resistance to system disturbances z.[8]

In order to perform simulations a 2nd order plant has been adopted, and limiting values of Δ_m perturbation have been evaluated for two confronted structures. As may be seen from Fig. 4, the n-MFC structure offers several times higher robustness to parameter variations than the classic single-loop PID structure. The robustness can be formed in different frequency ranges by an appropriate choice of R_k controller parameters.

IV. STABILITY

As may be easily noted in Fig. 2, the proposed control structure is composed of single-loop systems that are appropriately linked together. That is why intuition suggests that the global stability of an n-MFC system will be secured if each of the model loops, and the loop containing the real process are stable. To convince oneself that this is true, let us find the characteristic equation of the structure under study.

https://doi.org/10.1017/S0263574704001043 Published online by Cambridge University Press

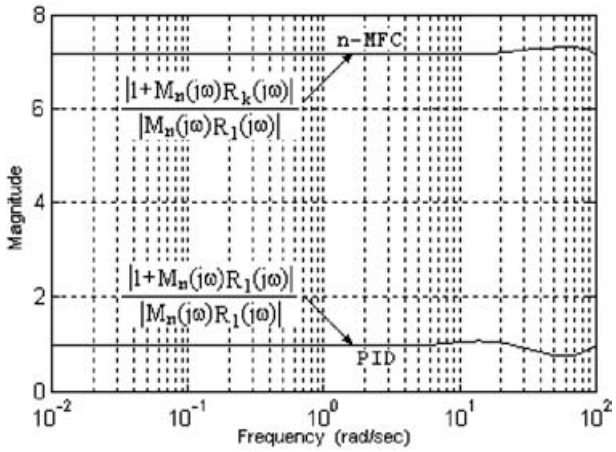


Fig. 4. Comparison of allowable perturbations of the classic PID system and the n-MFC structure.

Because of a less complicated mathematical description, we employ the corrective error value for the purpose of stability analysis. The structure depicted in Fig. 2 is described by the following system of equations

$$\begin{aligned} y &= P \cdot u \\ u &= u_n + R_k \cdot e_k \\ e_k &= y_{m1} - y \end{aligned} \tag{12}$$

which yield in

$$e_k = \frac{y_{m1} - Pu_n}{1 + PR_k} \tag{13}$$

Let the individual terms in the right-hand side of (13) be given as rational functions:

$$\begin{aligned} P &= \frac{l_K}{m_K}, \quad R_k = \frac{l_R}{m_R} \\ y_{m1} &= \frac{l_y}{m_y}, \quad u_n = \frac{l_u}{m_u} \end{aligned} \tag{14}$$

Substitution of (14) into (13) results in

$$e_k = \frac{m_R(l_y m_K m_u - l_K l_u)}{m_y m_u (m_K m_R + l_K l_R)} \tag{15}$$

By equating the denominator of (15) to zero we obtain the required characteristic equation of the n-MFC system, which represents a sole source of information about necessary conditions for system stability. As may be inferred from (15), the n-MFC structure is stable if the polynomials $m_y m_u (m_K m_R + l_K l_R)$ are Hurwitz ones, i.e. the real part of their every zero is negative. As one might expect, the stability of the first loop output y_{m1} and the stability of the manipulated variable u_n are required along with a stable corrective loop. Just as stability of the output y_{m1} in the classic feedback system remains beyond question, so does the provision of stability for u_n, which is described below.

$$u_n = y_o \frac{R_1}{\prod_{i=1}^{n}(1 + R_i M_i)} + y_{m1} \sum_{i=2}^{n} \frac{R_i}{\prod_{i}^{n}(1 + R_i M_i)} \tag{16}$$

Substitution of the equalities

$$M_i = \frac{l_{Mi}}{m_{Mi}}, \quad R_i = \frac{l_{Ri}}{m_{Ri}} \tag{17}$$

into (16) yields the characteristic equation for the simulated n-loops of the following form:

$$\prod_{i=1}^{n} (m_{Mi} m_{Ri} + l_{Mi} l_{Ri}) = 0 \tag{18}$$

According to (18), in order to provide a stable manipulated variable u_n, it is necessary that each simulated loop inclusive of the first reference loop is stable. Since a stable output y_{m1} is required for the first loop, and so is the manipulated variable u_1, hence, it may be concluded that the global stability of the n-MFC system depends not only on the stability of individual loops, but also on the stability of the model M_1.

V. ROBOTIC MANIPULATOR APPLICATION

Using the MFC structure proves itself first and foremost when we deal with a highly nonlinear process where classic control structures are not feasible to provide the required control performance. To test the proposed n-MFC system a robotic manipulator seems to be an ideal object. Due to its strong static and dynamic nonlinearities, as well as its nonstationarity, single-loop PID control systems are impractical for use here. Below the general form of the manipulator model will be presented.

Modeling the dynamics of a kinematic chain (Fig. 5) is more interesting from the viewpoint of control because the inverse model is easier to obtain than the forward one. Employing either the Newton-Euler approach or the Lagrange one[9] leads to a general equation of dynamics, which, after adding a term correcting for (viscous) friction, takes the form:

$$\boldsymbol{\tau} = \mathbf{M}(\mathbf{q})\ddot{\mathbf{q}} + \mathbf{C}(\mathbf{q}, \dot{\mathbf{q}}) + \mathbf{G}(\mathbf{q}) + \mathbf{F}(\dot{\mathbf{q}}) \tag{19}$$

where M is the $n \times n$ manipulator inertia matrix, C is the $n \times n$ matrix of velocity effect (centrifugal and Coriolis

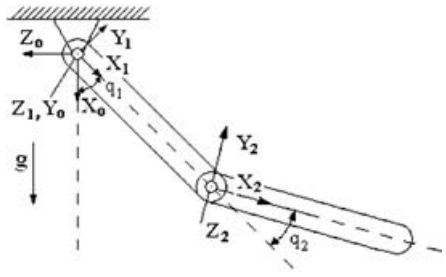


Fig. 5. Two-link robot arm with assigned coordinates.

https://doi.org/10.1017/S0263574704001043 Published online by Cambridge University Press

Table 1. Basic technical data of the EDDA manipulator.

Joint 1	
Construction	made of steel
Length of the arm	$l_1 = 0.3\,\text{m}$
Total mass	$m_1 = 20.7\,\text{kg}$
Type of the drive	direct, NSK Megatorque-Motor, $\tau_{1max} = 250\,\text{Nm}$ mass: $m_{S1} = 57\,\text{kg}$
Joint 2	
Construction	made of aluminum
Length of the arm	$l_2 = 0.5\,\text{m}$
Total mass	$m_2 = 2.2\,\text{kg}$
Type of the drive	direct, NSK Megatorque-Motor, $\tau_{2max} = 40\,\text{Nm}$ mass: $m_{S2} = 14\,\text{kg}$

torques), G is the $n \times 1$ vector of gravitational torque, F is the $n \times 1$ vector of friction force, τ is the $n \times 1$ vector of joint torque, q are the $n \times 1$ vectors of the joint displacement, velocity and acceleration terms, respectively.

It should be noted that eq. (19) represents an inverse model of the manipulator's dynamics. Since n-MFC employs a forward model, eq. (19) has to be rearranged to a useful form. Considering that the inertia matrix $M(q)$ is symmetrical and positive the forward model sought for may be written as:

$$\ddot{\mathbf{q}} = \mathbf{M}^{-1}(\mathbf{q})[\tau - \mathbf{C}(\mathbf{q}, \dot{\mathbf{q}}) - \mathbf{G}(\mathbf{q}) - \mathbf{F}(\dot{\mathbf{q}})] \qquad (20)$$

As is evident from eq. (20), model outputs are represented by accelerations for individual manipulator arms. To evaluate those, an access to velocities and positions is required. The two missing state variables can be obtained by a double integration of each of the terms.[10] Thus, the model obtained is the starting point to create the n-MFC structure.

V.1. Experimental setup

The n-MFC robot control system has been tested on the Experimental Direct Drive Arm EDDA, a two-joint robot arm (see Figure 6). Parameters of the manipulator are summarized in Table I. EDDA permits producing very high accelerations and velocities. On account of direct drives some properties are different to classic robots. Essentially, friction, torque and joint dynamics are meant here. This, however, is immaterial because, for example, position dependent loads, dynamic couplings and varying moments of inertia still exist.

MATLAB/SIMULINK has been used as basis software for implementing the algorithm, simulation and experiments. The system has been connected with the "real world" through the RT-Opal program and an I/O card operated under the QNX real-time operating system. Data exchange between the Matlab software (Windows-NT) and the QNX system took place via the TCP/IP protocol with the I/O card being connected with robot drives and sensors through signal matching. Fig. 6 depicts the principle drawing of the setup.

Not only dynamic, but also static nonlinearities exert an effect on the control performance. Above all, gravitation and friction are responsible for this. It may be easily noticed in Fig. 7 and Fig. 8.

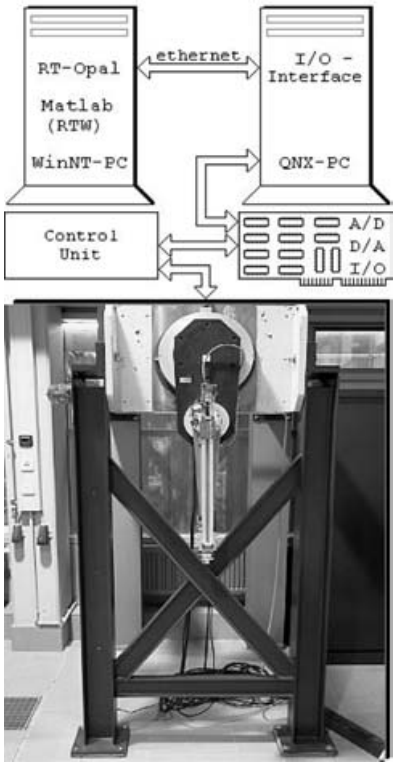


Fig. 6. The experimental setup.

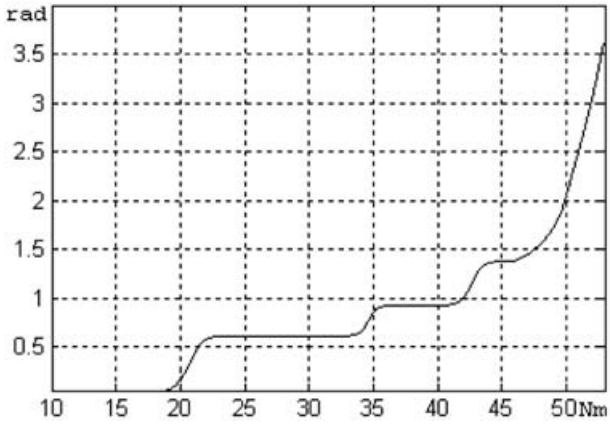


Fig. 7. Static characteristic of the first joint.

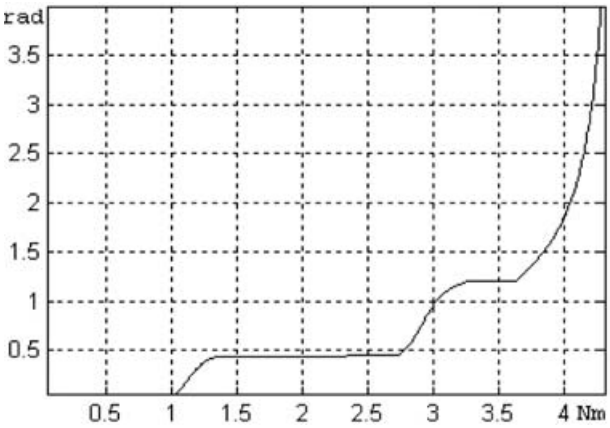


Fig. 8. Static characteristic of the second joint.

https://doi.org/10.1017/S0263574704001043 Published online by Cambridge University Press

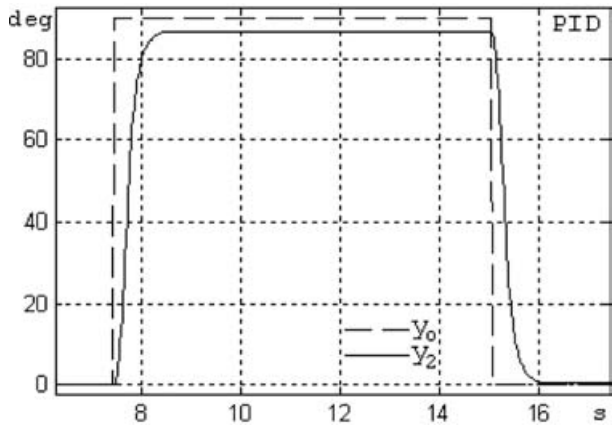


Fig. 9. Tuning of the controller (Joint 2).

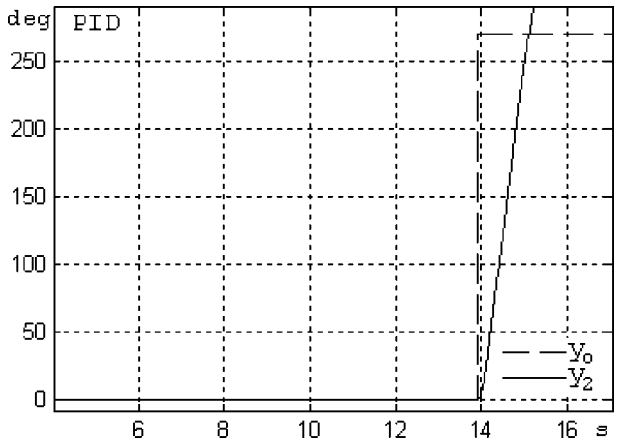


Fig. 10. Tuning of the controller. Loss of stability while changing the operating point (Joint 2).

V.2. Experimental results

In this section results of an experimental comparison drawn between three control structures, i.e. classic PID, two-loop MFC and three-loop 2-MFC, are presented. We began with tests carried out on a single-loop system. The controllers were tuned by experiment beginning with EDDA's second joint. As the operating point 0° and 90° have been chosen. Requirements to the control system were that the system should exhibit an aperiodic response, lack of the steady-state error and the shortest possible settling time.

The greatest difficulties in parameter tuning were caused by the integral part. The manipulator shows strong static nonlinearities. A single joint, for example, exhibits integrating properties at 0° and ±180°, and strong differentiating properties at ±90° and ±270°. For this reason, a compromise solution is necessary here. Considering that an aperiodic nature of the response has priority over the lack of steady-state error in the performance criterion adopted, the integral time constant was reduced, which yielded a response shown in Fig. 9.

The nonlinear nature of the control plant may account for the change in control performance while changing the operating point. The process turned out to be so complicated that the classic feedback control system could not ensure the system stability at demanded rise times (Fig. 10). The same applies to the first joint (Fig. 11).

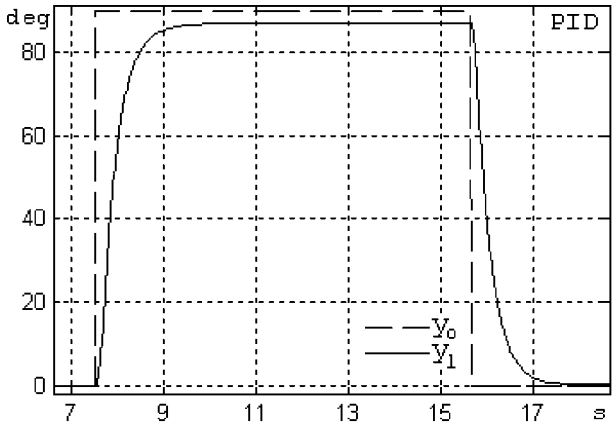


Fig. 11. Effect of dynamic couplings (Joint 1).

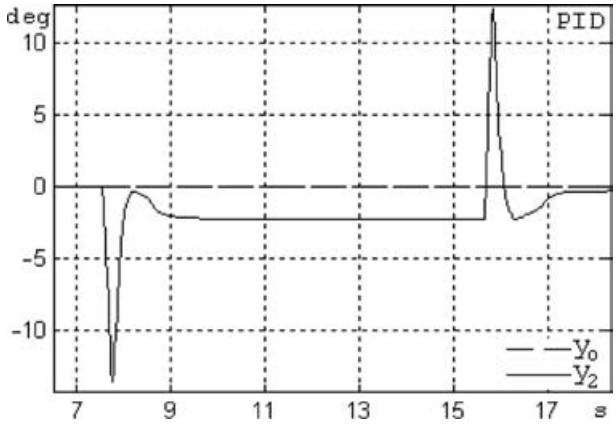


Fig. 12. Effect of dynamic couplings (Joint 2).

Below results of an experiment are presented, where the set-point was equal to 0°. Here the main objective was to investigate the effect of dynamic couplings on the control performance in the loop embracing the second joint.

High torques and accelerations produced by direct drives account for adverse phenomena occurring in the control system under study (Fig. 12). Remembered that the system can also lose its stability (Fig. 10); employing the classic PID control here becomes doubtful. Therefore, more advanced solutions are needed to get the demanded control performance. The Model-Based Control (MBC) systems[11] that employ either reverse process models or actual ones may offer an alternative here. In what follows, are results of tests carried out on the Model Following Control (MFC) system belonging to the MBC family.

Employing the complete manipulator model (20) in the first MFC loop turned out to be impossible. Too complicated nonlinear relationships of the dynamic model (20) precluded a satisfying control performance in the model loop of MFC. So, the model M_1 has been simplified to the form:

$$\ddot{\mathbf{q}} = \mathbf{M}^{-1}(\mathbf{q})[\tau - \mathbf{F}(\dot{\mathbf{q}})] \tag{21}$$

The model (21) has been implemented in a two-loop MIMO (Multiple Input Multiple Output) control system (Fig. 1). Tuning of the model controllers was performed by simulation, and that of the corrective controllers was carried

https://doi.org/10.1017/S0263574704001043 Published online by Cambridge University Press

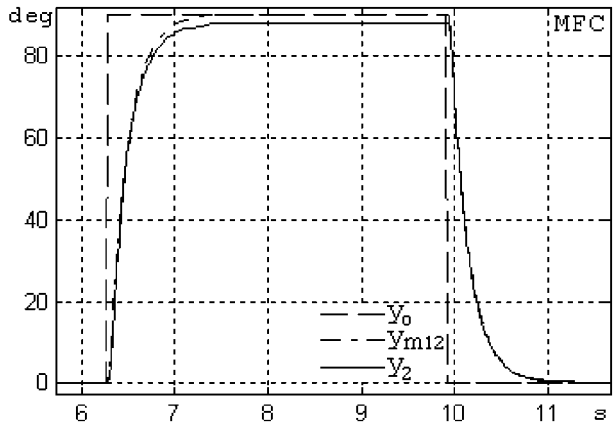


Fig. 13. Tuning of the controller (Joint 2).

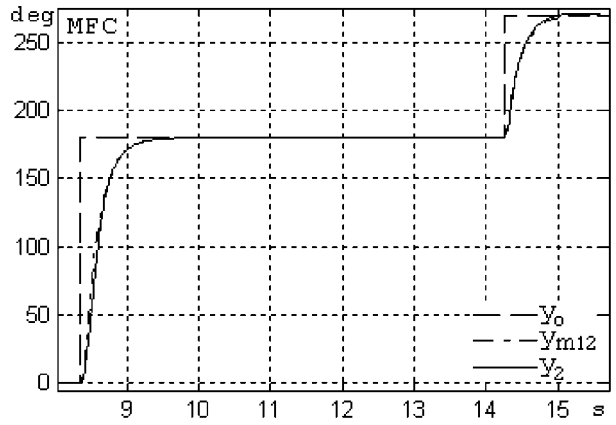


Fig. 14. Tuning of the controller. Control performance when the operating point is changed (Joint 2).

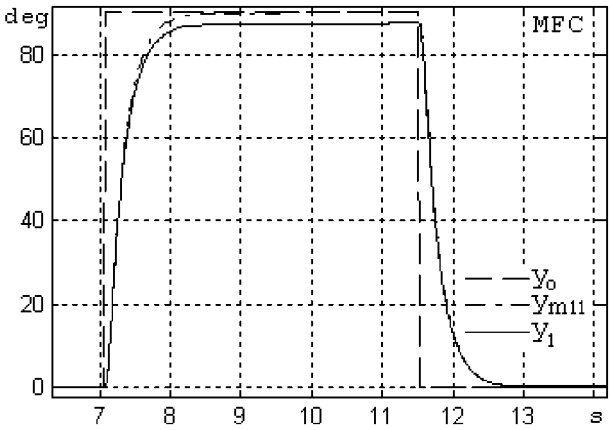


Fig. 15. Effect of dynamic couplings produced by the second joint on the first one.

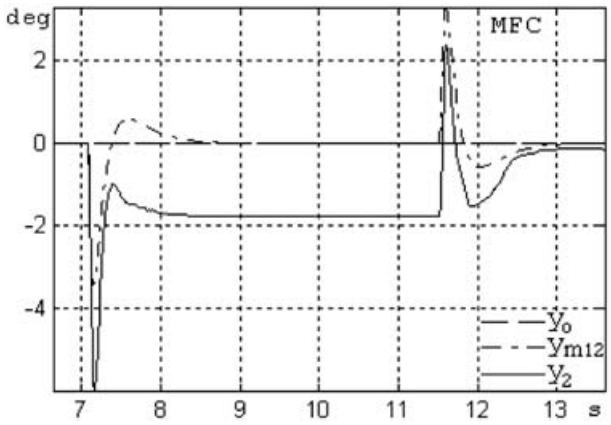


Fig. 16. Effect of dynamic couplings produced by the first joint on the second one.

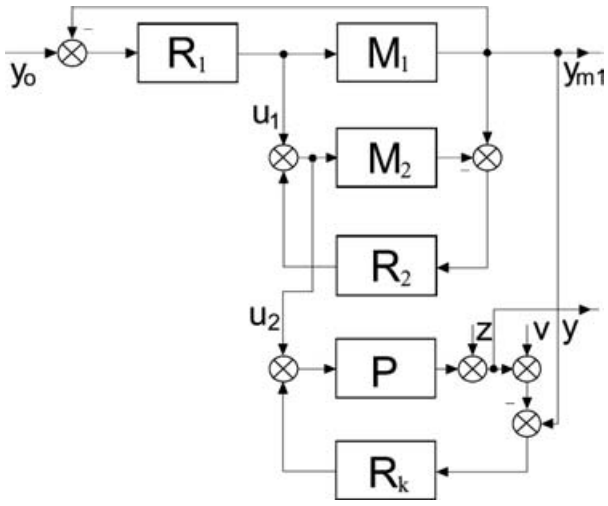


Fig. 17. Structure of the 2-MFC system.

out by experiment. As in the case of the classic feedback systems, the tuning started with the second joint for the same operating point (Fig. 13).

As may be inferred from Figs. 9 and 13, it is scarcely possible to assess, whether employment of MFC is beneficial. However, this control technique makes it possible to keep the system stability even if the operating point is changed, i.e. for an arbitrarily chosen set-point (Fig. 14). An improved control performance is also visible in the case of occurring dynamic couplings (Fig. 12 and Fig. 16). But for a shift between the model output y_{m12} and the plant output y_2 resulting from the existing steady-state error (Fig. 16), amplitudes here are very close to those occurring in the model M_1. This adverse effect can be reduced, for example, by increasing the friction factor of the model M_1.

The only drawback in the control performance yielded by MFC is the steady-state error, which occurs wherever a great deal of energy is needed to be delivered to keep the manipulator in a required position (Figs. 15 and 16). Since the model M_1 takes no account of gravitation, the corrective controller R_k tried to cope with this phenomenon. However, too strong process nonlinearities prevented even the two-loop MFC structure from satisfying the conditions of the demanded control performance. A three-loop 2-MFC with an additional model loop could manage to cope with the problem of the adverse effect the static nonlinearities exert on the control performance (Fig. 17).

To make use of a multi-loop n-MFC, the process model is split and written in the general form of eq. (3). In this specific

https://doi.org/10.1017/S0263574704001043 Published online by Cambridge University Press

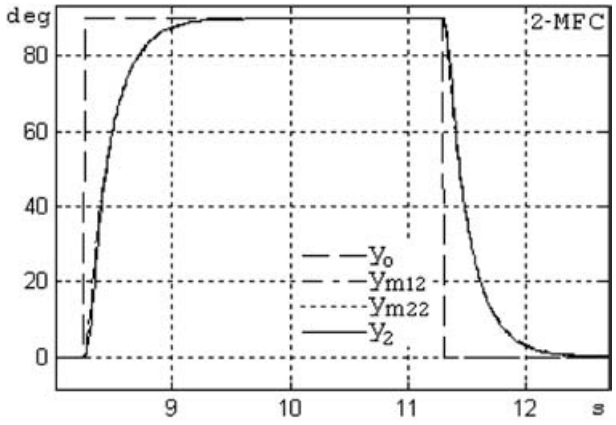


Fig. 18. Tuning of the controller (Joint 2).

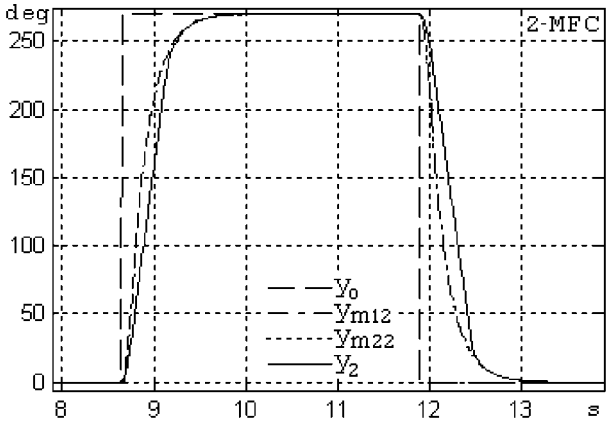


Fig. 19. Tuning of the controller. Control performance at the other operating point (Joint 2).

case of two presimulated loops the models M_1 and M_2 are

$$\begin{aligned} M_1 \Rightarrow \quad & \ddot{\mathbf{q}} = \mathbf{M}^{-1}(\mathbf{q})[\tau - \mathbf{F}(\dot{\mathbf{q}})] \\ M_2 \Rightarrow \quad & \ddot{\mathbf{q}} = \mathbf{M}^{-1}(\mathbf{q})[\tau - \mathbf{C}(\mathbf{q}, \dot{\mathbf{q}}) - \mathbf{G}(\mathbf{q}) - \mathbf{F}(\dot{\mathbf{q}})] \end{aligned} \tag{22}$$

For a such split model, a three-loop 2-MFC structure (Fig. 17) has been implemented and parameterized. Tuning of the controllers serving the M_1 and M_2 models was performed by simulation, and that of the corrective controllers was carried out by experiment. As before, the process of tuning started with the second joint of the manipulator.

As can be inferred from Fig. 18, the additional presimulated loop ensures an aperiodic response that is also free of a steady-state error. The same control performance can also be observed at other operating points of the system (Fig. 19). Positive results were also obtained for the first joint of the EDDA manipulator (Fig. 20).

Figure 21 illustrates the effect of couplings that have experienced a slight increase (Figs. 16 and 21) despite higher friction factors in M_1 and M_2 due to selection of a lower gain of corrective controllers in 2-MFC. However, selection of appropriate high gains for R_k results in that the model M_1 tracking is improved, and the adverse effect of couplings is reduced.

In the multi-loop control structure each loop produces a certain nonlinear component of the manipulated variable.

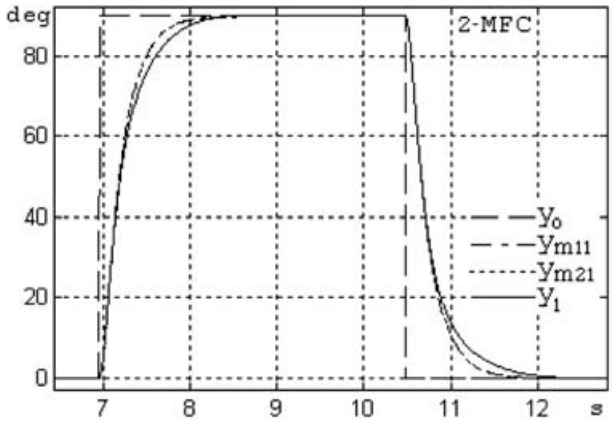


Fig. 20. Effect of dynamic couplings produced by the second joint on the first one.

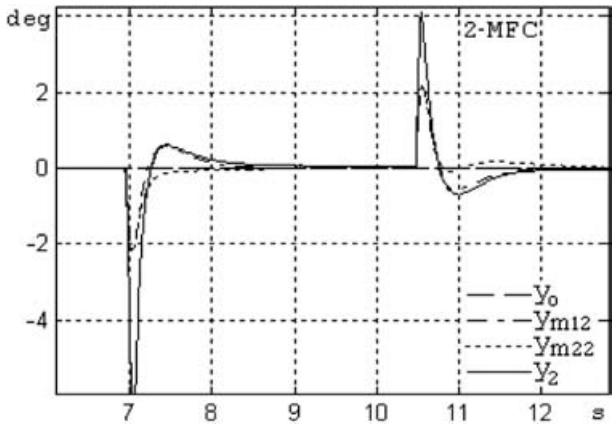


Fig. 21. Effect of dynamic couplings produced by the first joint on the second one.

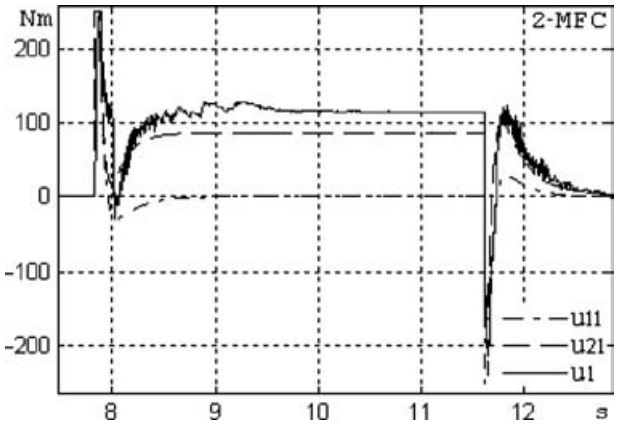


Fig. 22. Manipulated variables in individual 2-MFC system loops (Joint 1).

The components are added up to form the global manipulated variable. In Figs. 22 and 23 controller outputs for two joints are exemplified. It can be observed here, how the form of the manipulated variable undergoes change, beginning from the simplest form, through a more nonlinear one, up to the general manipulated variable u.

A comparison of responses obtained for MFC and 2-MFC leads us to a notice that the latter structure provides a smaller steady-state error than the former. The value of the error has

https://doi.org/10.1017/S0263574704001043 Published online by Cambridge University Press

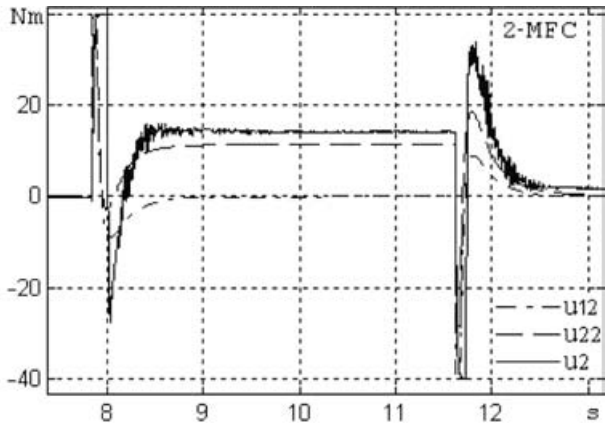


Fig. 23. Manipulated variables in individual 2-MFC system loops (Joint 2).

been reduced from several degrees for MFC up to 0.1° for 2-MFC. The additional loop enables one to utilize the available process model more effectively, and to generate an additional nonlinear component of the manipulated variable.

VI. CONCLUSIONS

Although exemplified by control of a manipulator, the multi-loop control system can find a much wider use in practice. Whether the two-loop MFC with a single model or the expanded three-loop 2-MFC system, it can be applied to a wide range of processes thanks to the frequently existing possibility of subdividing the process model into its static and dynamic part while creating the model. It also should be stressed here, that the solution under discussion remains unchanged from the viewpoint of its structure and parameters, which is an advantage, and thus, presents an alternative to more complicated and expensive adaptive systems.

In the paper results of experimental tests carried out on n-MFC structures, that are based on an accurate process model have been presented. The effect of model inaccuracy or system robustness has not been evaluated yet. However, the robustness of a two-loop MFC structure was analyzed in [5], where the two-loop MFC system with compensated gravitation has been confronted with the well-known feedforward system.

Acknowledgment

This research was supported by KBN (Polish State Committee for Scientific Research) under Grant No. 3 T11A 009 26 and by the German Science Foundation DFG.

References

1. Mareels I. and Polderman J. W.: *Adaptive Systems: An Introduction* Birkhäuser, Boston, 1996.
2. Li G., Tsang K. M. and Ho S. L.: *A novel model following scheme with simple structure for electrical position servo systems*. International Journal of Systems Science, 29, 1998, pp. 959–969.
3. Skoczowski S. and Domek S.: *Robust Model Following PID Control*. Proc. 14 th International Conference on Systems Science, 11–14 September 2001, Wrocław, Poland, Vol. II, pp. 54–61.
4. Skoczowski S.: *Robust Model Following Control With use of Plant Model*. International Journal of Systems Science, 2001, Taylor & Francis LTD, Vol. 32, no. 12, pp. 1413–1427.
5. Osypiuk R., Finkemeyer B. and Wahl F. M.: *Forward-Model-Based Control System for Robotic Manipulators*. Robotica, Cambridge University Press, Vol. 22, No. 2, Mar 2004, pp. 155–161.
6. Osypiuk R.: A *Novel Multi-loop Control System for Highly Nonlinear Processes*, Systems Science, Vol. 29, No. 4, 2003, pp. 43–54.
7. Geering H. P.: *Robuste Regelung*, Institut für Mess- und Regeltechnik Eidgenössische Technische Hochschule, Zürich, 2. Auflage, März 1999.
8. Ludyk G.: *Theoretische Regelungstechnik 2,* Springer 1995.
9. Spong, M. W. and Vidyasagar, M.: *Robot Dynamics and Control*, John Wiley & Sons, New York, 1989.
10. Craig J. J.: *Introduction to robotics: mechanics and control* 1986, Reading, Mass.: Addison-Wesley.
11. Albertos P.: *Weighted model-based control*, European Control Conference ECC'93, Groningen, The Netherlands, 1993, pp. 1935–1939.

https://doi.org/10.1017/S0263574704001043 Published online by Cambridge University Press